Quasi-Band Electronic Structure of V n (benzene) n+1 Clusters

ARTICLE *in* THE JOURNAL OF PHYSICAL CHEMISTRY A · MAY 2002

Impact Factor: 2.69 · DOI: 10.1021/jp020494h

Quasi-Band Electronic Structure of $V_n(benzene)_{n+1}$ Clusters†

Ken Miyajima, Kazuhiko Muraoka, Masatomo Hashimoto, Tomokazu Yasuike,‡ Satoshi Yabushita, and Atsushi Nakajima*

Department of Chemistry, Faculty of Science and Technology, Keio University, 3-14-1 Hiyoshi, Kohoku-ku, Yokohama 223-8522, Japan

Koji Kaya*

Institute for Molecular Science, Myodaiji, Okazaki 444-8585, Japan

Received: February 21, 2002; In Final Form: May 9, 2002

Photoionization efficiency (PIE) curves were measured for sandwich vanadium−benzene clusters, $V_n(benzene)_{n+1}$ ($n = 1-5$), which were produced by the reaction of laser-vaporized vanadium atoms with benzene vapor. A two-rod laser vaporization source was used for enhancing the production of the larger clusters. The second lowest ionization energies of the sandwich clusters were probed experimentally for the first time. The PIE curves of the sandwich clusters clearly present evidence that the clusters take a quasi-band electronic structure which results from a one-dimensional sandwich structure.

1. Introduction

Metal−ligand molecules have been the subject of many studies in the past decade.[1−6] Clusters (complexes) of transition-metal atoms and benzene molecules have been the focus of much of this research because they provide basic models for d−π bonding interactions. In particular, the metal−ligand sandwich systems have attracted the attention of scientists for a half century following the discovery of ferrocene, $Fe(\eta^5\text{-}C_5H_5)_2$. In related work, a few examples of the synthesis of triple-decker sandwich complexes composed of transition-metal atoms and Cp ligands such as $Ni_2Cp_3^+$ (in the bulk)[7] and $Fe_2Cp_3^+$ (in the gas phase)[8] have been reported, and these have attracted much attention for the detailed study of metal−metal interactions in organometallic systems. Interestingly, it has been shown that these one-dimensional stacking compounds can exhibit semiconducting or even conducting properties in the solid state.[9,10]

Although many synthetic experiments have been conducted on novel organometallics in the condensed phase, various environmental factors such as oxidation or reduction of the products make these approaches problematic. Since the advent of laser and molecular beam techniques, gas-phase experiments have offered ideal environments for detailed investigations of chemical reactions of metal ions.[11] Furthermore, gas-phase experiments enable us to make novel complexes and to use several powerful spectroscopic means.[12,13] One of the advantages of gas-phase synthesis is the exclusion of environmental factors such as counterions and solvent molecules. In addition, in some cases removal of solvent and counterions can stabilize the molecule against nonradiative decay processes, allowing excited electronic state properties to be probed. For example, some groups have investigated the reactivity of neutral metal atoms toward small hydrocarbon molecules, and they made clear that each electronic state exhibits different chemistry.[14,15]

Recently, we have synthesized vanadium−benzene clusters using a combination of the laser vaporization and molecular beam methods in the gas phase.[13,16,17] From the observed magic numbers and other experimental properties (reactions with CO gas and ion mobilities)[16−18] and theoretical studies,[19,20] these clusters were assumed to have a multiple sandwich structure, in which metal atoms and benzene molecules are alternately stacked in a one-dimensional structure.

Among the physical properties of the cluster, photoionization behavior is one of the most important, because it provides information on both the electronic and the geometrical structure.[21−23] The cluster size dependence of the ionization energy provides a quantitative measure of the evolution of electronic structures, which can be directly compared to theoretical predictions. For vanadium−benzene clusters, in particular, the ionization energies of the clusters drop significantly with increasing cluster size.[17] This tendency has been successfully explained by Yasuike et al. as the delocalization of d electrons along the molecular axis.[20] The bonding orbitals are formed mainly between d_δ (V atom) and L_δ (benzene) orbitals, respectively. Qualitatively, increasing the size of the multiple-decker sandwich clusters leads to the formation of quasi-band electronic structure of these bonding orbitals by one-dimensional delocalization of the d_δ electrons. The lowest energy ionization process corresponds to ionization from the upper end of the d_δ band.

In this study, the photoionization efficiency (PIE) curves for the multiple-decker sandwich clusters are measured to investigate the quasi-band electronic structure, using a new cluster enhancement technique based on laser vaporization of a double rod source. The second ionization threshold is found as a second onset in the PIE curve, and the values obtained are compared with theoretical predictions.

2. Experimental Section

Details of the experimental setup have been described elsewhere.[13,17] Briefly, $V_n(C_6H_6)_m$ clusters were synthesized by the reaction of laser-vaporized metal atoms and benzene

† Part of the special issue "R. Stephen Berry Festschrift".

* To whom correspondence should be addressed: E-mail: nakajima@sepia.chem.keio.ac.jp or kaya@ims.ac.ip.

‡ Present address: Graduate School of Arts and Sciences, the University of Tokyo, 3-8-1 Komaba, Meguro-ku, Tokyo, 153-8902, Japan.

10.1021/jp020494h CCC: $22.00
Published on Web 08/27/2002

molecules. In the cluster source chamber, two vanadium rods (5-mm diameter, purity 99.8%) were vaporized by the tightly focused second harmonic output (532 nm) of two pulsed Nd^{3+}: YAG lasers (New Wave Research Inc., Tempest-30, 532 nm, 3−5 ns pulse width). The rods were simultaneously rotated and translated within a stainless steel block in order to avoid drilling a hole in the sample. The distance between the two laser vaporization spots on the target rods was 4 mm. Vaporized hot metal atoms were cooled by pulsed He carrier gas (purity 99.9999%, ∼6 atm backing pressure). The cooled vanadium atoms were sent into a flow-tube reactor where the saturated benzene vapor seeded in a He gas (1.5−2 atm; room temperature) was injected in synchronization with the pulsed flow. The diameter of the channel inside the reactor was 3 mm.

The generated $V_n(C_6H_6)_m$ clusters were sent into the ionization chamber through a skimmer. Typical background pressure in the ionization chamber was $\sim 3 \times 10^{-6}$ Torr. The photoionization of these clusters was performed in the extraction region of a reflectron time-of-flight (RTOF) mass spectrometer. The photoions formed from the neutral clusters were accelerated by the static extraction field (3 kV) and were sent into the RTOF mass spectrometer. Signals were detected from a scintillation ion detector of the modified Daly type (the Even cup), operated in conjunction with a fast photomultiplier tube.[24−26]

The cluster beam was intersected with two ionization laser beams in the same space. One is an ArF excimer laser (193 nm, 6.42 eV; Lambda Physik LPX110i), and the other is a tunable laser pulse from an optical parametric oscillator (MOPO-730, Spectra Physics). The ArF excimer laser provides photons of sufficient energy to ionize any of the vanadium−benzene clusters in a one-photon process. This is employed to measure a reference signal, which is used to correct for shot-to-shot fluctuations in cluster density. The second harmonic output of OPO laser (340−220 nm) or its mixing output with the fundamental of a Nd^{3+}:YAG laser (240−193 nm) was used as a "probe" laser. The wavelength of the probe laser was varied in intervals of 2 or 4 nm (about 0.02−0.05 eV). The fluences of the both the ArF laser and the tunable ultraviolet laser were monitored by two independent pyroelectric laser energy detectors (Molectron, J3−05) following transmission through the instrument. Laser fluences were typically kept near 200 μJ/cm^2 to avoid multiphoton processes. Under this condition of low laser fluence, the ionization process occurs independently for the two lasers without any multiphoton processes.

The PIE curves for (n, $n+1$) of the vanadium−benzene clusters ($n = 1-3$) were previously measured for a limited energy region around their lowest ionization energies.[19] However, it is generally difficult to measure PIE curves for a wide energy range, because fluctuation in the cluster abundance make small features difficult to detect. Therefore a particular stable source is indispensable if one hopes to detect the second ionization threshold in the PIE curves. Two improvements were made in this experiment to measure reliable PIE curves; The first enhanced and stabilized the production of larger clusters via a two-rod vaporization source. The second corrected for shot-to-shot fluctuations by measuring the relative cluster concentration on every shot.

In this work, both of the lasers used for ionization were intersected with the cluster beam in the same space with a short delay between them (for example, ∼0.6 μs). This technique can effectively cancel out the fluctuations in the cluster abundance.[27,28] The normalized photoionization intensity I_{eff} of a certain cluster is evaluated by the ratio of the signal intensity I_{OPO} to the signal intensity I_{ArF} including the normalization of laser fluence of the probe and the reference lasers. The laser fluence is calculated from the outputs of the pyroelectric detectors (E_{OPO}, E_{ArF}) and the wavelength of the ionization lasers. Since a pyroelectric detector measures the total energy incident on it, this may be converted to a value proportional to the number of photons using the wavelength. The abundances of photoions were obtained from the peak intensity of a certain cluster in a TOF spectrum (I_{OPO}, I_{ArF}). Thus, the photoionization intensity I_{eff} can be written as

$$I_{\text{eff}} = \frac{I_{\text{OPO}}/E_{\text{OPO}}}{I_{\text{ArF}}/E_{\text{ArF}}} \cdot \frac{\lambda_{\text{ArF}}}{\lambda_{\text{OPO}}} \qquad (1)$$

where λ_{OPO}, λ_{ArF} are the wavelengths of each laser.[23] A PIE curve was plotted against photon energy. The ionization energy (E_i) was evaluated by extrapolating the first linear rise in the PIE curve to the baseline.[21,22] The fitting error is mainly due to the uncertainty in the determination of linear increase of PIE curves and is estimated to be about 0.05 eV.

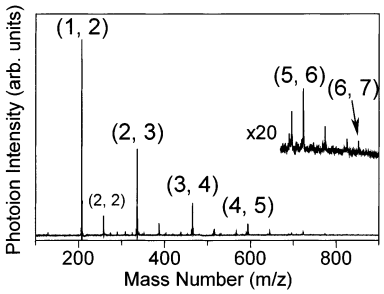

Figure 1. Typical time-of-flight spectrum for $V_n(C_6H_6)_{n+1}$ clusters ionized by 193 nm (6.42 eV). Peaks are labeled according to the notation $V_n(C_6H_6)_m = (n, m)$, where the prominent series of (n, $n+1$) is assigned as multiple-decker sandwich clusters. Using two-rod vaporization, the production of larger clusters was significantly enhanced.

3. Results and Discussion

3.1. Enhanced Cluster Production by Two-Rod Vaporization. In this section, the effect of the metal vapor concentration on cluster abundance is discussed to obtain insight into how the vanadium−benzene clusters are produced. Figure 1 shows the photoionization TOF spectrum of $V_n(C_6H_6)_m$. The abbreviation of (1, 2) means that this cluster consists of one vanadium atom and two benzene molecules. The predominant peaks have magic numbered compositions of (n, $n+1$), and most of the minor peaks are assigned to the (n, n) clusters. Together with other experimental and theoretical studies, [13,16−20] strong evidence exists that the clusters have a sandwich structure at (n, $n+1$), where vanadium atoms and benzene molecules are alternately piled up.

As shown in Figure 1, the intensities of the vanadium−benzene sandwich clusters in the mass spectrum decrease with cluster size. To measure electronic properties, the abundance of the lager clusters must be increased sufficiently for accurate measurements. When the partial pressure of benzene vapor was increased by heating the benzene reservoir from 300 to 330 K, the mass spectrum was unchanged. On the other hand, a higher concentration of V atom vapors produced by laser vaporization of two rods sufficiently increased the cluster concentrations; the combination of up- and downstream laser vaporization gains much more clusters than the sum of the individual laser vaporization processes, especially for the larger cluster sizes. This result indicates that the production of V atoms is the rate-determining step, while the benzene vapor is in excess.

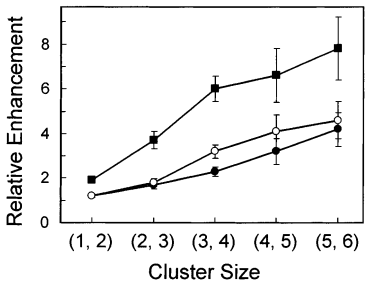

Figure 2. Laser power dependence of the enhancement of two-rods vaporization for the production of $V_n(C_6H_6)_{n+1}$. The intensity ratio between (a) the summation of single-rod independent vaporizations and (b) two-rod simultaneous vaporization, calculated as (b)/(a), was evaluated for each cluster size. When there is no enhancement using the two-rod vaporization source, the value of (b)/(a) becomes 1. Solid circles, open circles, and solid boxes indicate the low (~4.5 mJ), intermediate (~4.8 mJ), and high (~5.0 mJ) laser power conditions, respectively. With increasing laser power, the production of the larger clusters is significantly enhanced.

Figure 2 shows the laser power dependence of the relative enhancement of the two-rod vaporization process for the production of vanadium−benzene clusters. Under the same production conditions, the cluster abundances were measured in the cases of (a) the summation of single-rod independent vaporizations and (b) two-rod vaporization. The signal plotted in Figure 2 as the relative enhancement is the ratio of the signals ($I_{\text{both}}/\{I_{\text{upstream}} + I_{\text{downstream}}\}$). The two-rod vaporization method significantly enhances the formation of the clusters, when the time delay between two vaporization lasers was set at 5 ± 1 μs. This time delay corresponds reasonably well to the time that it takes for the He gas to flow from one rod to the other (4 mm separation) for a helium flow velocity of about 800 m/s in the channel.

The different symbols plotted in Figure 2 provide the enhancement factors obtained at different vaporization laser energies. Solid circles, open circles, and solid boxes indicate the low (~4.5 mJ), intermediate (~4.8 mJ), and high (~5.0 mJ) laser power conditions, respectively. With increasing laser power, the abundance of the larger cluster is considerably enhanced. Above 5.5 mJ, however, the cluster intensity dropped, presumably because the helium was incapable of cooling the clusters adequately under these conditions.

In this experimental setup, the vanadium−benzene clusters are generated inside the fast-flow reactor. If the formation reaction is of multiple order, the higher concentration of vanadium atoms produced using the two-rod source should yield more products than the sum of the products formed in the two single-rod sources. Indeed, the cluster abundance was increased more than the sum, especially in large sandwich clusters. Then, the V vapors from two laser-vaporization processes were evidently supplied into a common cluster growth region, allowing more effective growth of the larger clusters. The high sensitivity to cluster abundance for the larger sizes indicates that they are produced through consecutive reactions with alternate additions of V atoms and benzene. Under conditions of excess benzene vapor, the reaction rate seems to be governed by the multiple-order of the vanadium atom concentration; the production rate is expected to be proportional to $[V]^n$ for production of the $(n, n + 1)$ cluster. Although this behavior is approximately found for small values of n, Figure 2 shows that the higher concentration of vanadium atoms does not necessarily accelerate the formation efficiency of larger clusters. This probably occurs because the contact period inside the reactor limits the production of larger clusters. In any case, the double-rod vaporization source enables us to produce considerably larger vanadium−benzene clusters, up to $n = 10$, and also enables us to measure the PIE curves of (4, 5) and (5, 6) as well as $(n, n + 1)$ for $n = 1-3$.

It is interesting to note that excited metal atoms are thought to be a key reactant for production of the sandwich clusters, although the electronic state population of laser vaporized metal atoms is not obvious. Yasuike et al. have given theoretical descriptions for the production efficiency for the transition-metal−benzene complexes.[19] According to their work, spin conservation is expected to dominate the sandwich growth process. As a result, excited atoms produced by laser vaporization are expected to play an important role in the reaction with benzene. Electronically excited metal atoms that have no electrons in the 4s orbital are likely to react more easily because of the unfavorable repulsion between electrons in the large 4s orbital and the benzene molecules is reduced. Furthermore, electronically excited atoms having lower electron spin preferably form complexes with benzene ligands through an electron-spin-conserved pathway, because the complexes in the ground state usually prefer to take a lower spin state. Indeed, the relative abundance for (1, 2) was slightly enhanced by laser vaporization with higher fluence, as indicated in Figure 2. From this point of view, it is expected that a population of vanadium atoms in electronically excited states is crucial for enhanced production of large sandwich clusters. Unfortunately, it is experimentally difficult to determine how many excited vanadium atoms survive until the reaction with benzene.

3.2. Photoionization Efficiency Curves and the Second Lowest Ionization Energies. *3.2.1. Photoionization Efficiency Curves.* With time-delayed probe and reference photoionization, the series of $(n, n + 1)$ clusters are observed as a sequence of ion pairs, where they were ionized by both the probe and the reference lasers. A time delay of ~0.6 μs between the probe and the reference lasers appears as the interval between each pair of peaks. The intensity ratio of the probe and reference signals reflects the photoionization efficiency for each size. Since the E_i of $(n, n + 1)$ decreases with increasing n, the intensity ratio of the probed ion to the referenced ion increases with the size. Figure 3 shows the PIE spectra for (1, 2) to (5, 6), where the cluster photoionization efficiency was plotted as a function of photon energy. The PIE was normalized at the photon energy of 6.42 eV. The first onset corresponds to the ionization threshold for removing an electron from the HOMO, giving the ionization energy, E_i. The E_i value was evaluated by extrapolating the first linear rise in the PIE curve to the baseline. The E_i of (5, 6) was obtained for the first time in this work. The E_i's of $(n, n + 1)$ for $n = 1-4$ are in agreement with those reported previously.

As well as the first onset, a second ionization onset was observed as the change of slope in the PIE curves of (3, 4) and (4, 5), as shown in Figure 3; the PIE curve rises up more conspicuously at higher photon energy. This second onset can be regarded as the opening of another ionization channel. Although the second onset for (5, 6) is somewhat obscure, the energies for the second onsets were obtained to be 5.8 ± 0.1, 4.9 ± 0.1, and 4.7 ± 0.1 eV for (3, 4), (4, 5), and (5, 6), respectively. The energy for the second onset decreases with cluster size, which is similar to the trend in the lowest ionization energy, E_i. The electronic features that were found as the first and the second onsets in the PIE curves can be explained by the following quasi-band model for one-dimensional sandwich clusters as ionization processes from the HOMO and the HOMO-1.

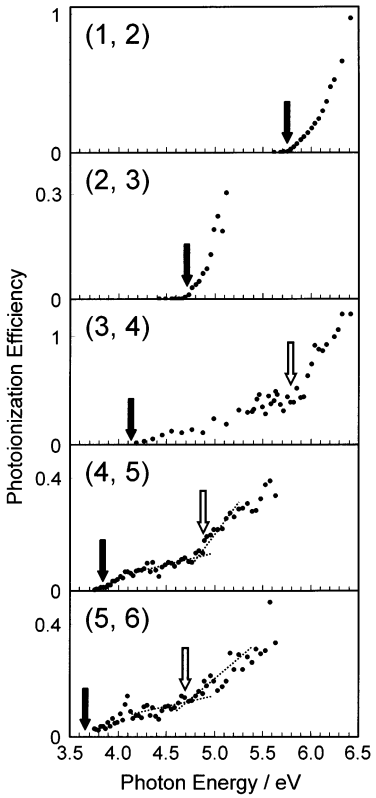

Figure 3. Photoionization efficiency curves for $V_n(C_6H_6)_{n+1}$ ($n = 1-5$). Solid and open downward arrows indicate the lowest and the second lowest ionization thresholds, respectively.

3.2.2. Analysis of the Quasi-Band Electronic Structure by Simple Hückel Model. The theoretical analysis of the E_is was carried out by applying the simple Hückel method to the one-dimensional Bz−V−Bz−V− ··· −V−Bz structure (Bz = benzene) as before.[20] As discussed there, charge-transfer interactions between the vanadium $3d_\delta$ orbital and benzene LUMO form quasi-band structures and are responsible for both the V−Bz bonding and the significant size dependence of lowest E_i. In the present study, we further enforce the above statement by comparing the experimental and theoretical quasi-valence-band structure. The Hückel Hamiltonian with these fragment orbitals in δ symmetry has the following simple form:

$$H = U\begin{pmatrix} 1 & \beta & & & & & & \\ \beta & 0 & \beta & & & & & \\ & \beta & 1 & \beta & & & & \\ & & \beta & \cdot & \cdot & & & \\ & & & \cdot & \cdot & \cdot & & \\ & & & & \cdot & \cdot & \cdot & \\ & & & & & \cdot & \cdot & \beta \\ & & & & & & \beta & 0 & \beta \\ & & & & & & & \beta & 1 \end{pmatrix} \quad (2)$$

where U is the orbital energy difference between the benzene LUMO and $3d_\delta$ and $U\beta$ is the resonance integral between these neighboring fragment orbitals. For simplicity, we set the orbital energy of $3d_\delta$ to be zero. It is straightforward to derive the following HOMO energies, $\epsilon_{HOMO}(n, n+1)$, from the above Hückel Hamiltonian:

$$\epsilon_{HOMO}(1,2) = \frac{1-\sqrt{1+8\beta^2}}{2}U \quad (3)$$

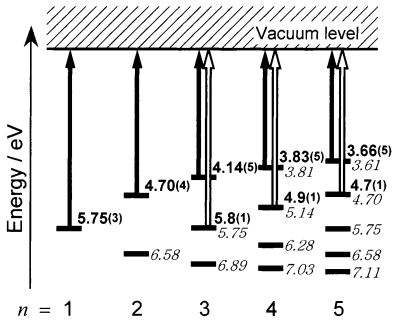

Figure 4. Quasi-band electronic structure of d_δ orbitals for $V_n(C_6H_6)_{n+1}$. Numbers in parentheses indicate experimental values in electronvolts with uncertainties; 5.75(3) represents 5.75 ± 0.03 eV. Calculated values obtained by the simple Hückel model are given in italics. Solid and open arrows indicate the lowest and the second lowest ionization processes, which were observed, respectively.

$$\epsilon_{HOMO}(2,3) = \frac{1-\sqrt{1+4\beta^2}}{2}U \quad (4)$$

and

$$\epsilon_{HOMO}(3,4) = \frac{1-\sqrt{1+(8-4\sqrt{2})\beta^2}}{2}U \quad (5)$$

With the experimental lowest E_is for $n = 1$, 2, and 3, shown in Figure 4, we can semiempirically determine the above Hückel parameters U, β, and the vacuum level position relative to the atomic $3d_\delta$ level, and U and β^2 evaluated are 2.766 eV and 0.9893. Having determined these parameters, we can obtain all the remaining eigenvalues for various cluster size. It is interesting to point out that the above simple Hückel method predicts that the next HOMO (HOMO-1) of (3, 4) and the HOMO of (1, 2) have identical energy. Therefore, the second lowest E_i for (3, 4) is expected to be similar to the lowest E_i for (1, 2). Likewise, the second lowest E_i for (5, 6) is expected to appear close to the lowest E_i for (2, 3).

Figure 4 summarized the experimentally obtained lowest and second lowest E_is in boldface along with the theoretical E_is calculated with this Hückel model and the Koopmans theorem in italics. The experimentally determined lowest E_is for (4, 5) and (5, 6) are well predicted by this simple model calculation. Furthermore, the positions of the second onsets in the PIE curves were consistent with the theoretical prediction for ionization from the next HOMO's. In fact, there is no orbital other than the d_δ orbitals in this energy region and splitting in the evolution of the d_σ orbitals is much smaller.[20] From these facts, the change in the slope of the curve can be reasonably ascribed to the second lowest ionization.

The differences between the experimentally and theoretically obtained values are somewhat larger in the case of the second lowest E_is. It seems that the experimental values for the second lowest E_is take slightly lower energy than the theoretical ones, and that they exhibit a difference of 0.24 eV for (4, 5). This may indicate that the assumption that all of the vanadium atoms and benzene molecules are located at an equal distance and are fixed on the molecular axis may be in error.

4. Conclusion

The $V_n(C_6H_6)_{n+1}$ clusters were produced by a combination of laser vaporization and molecular beam methods. The two-rod laser vaporization source enabled us to enhance the production of larger vanadium−benzene clusters. The photo-

ionization efficiency curves obtained for the (3, 4), (4, 5), and (5, 6) clusters indicated the presence of another ionization channel from the next HOMO orbital (HOMO-1). This result can be regarded as clear experimental evidence that the vanadium−benzene clusters have a quasi-band electronic structure with multiple-decker sandwich structures.

Acknowledgment. This work is supported by a program entitled "Research for the Future (RFTF)" of the Japan Society for the Promotion of Science (JSPS) (98P01203). K. Miyajima and T. Yasuike express their gratitude to Research Fellowships of the JSPS for Young Scientists.

References and Notes

(1) Kealy, T. J.; Pauson, P. L. *Nature (London)* **1951**, *168*, 1039.
(2) Miller, S. A.; Tebboth, J. A.; Tremaine, J. F. *J. Chem. Soc.* **1952**, 632.
(3) Muetterties, E. L.; Bleeke, J. R.; Wucherer, E. J.; Albright, T. A. *Chem. Rev.* **1982**, *82*, 499.
(4) *Comprehensive Organometallic Chemistry*; Wilkinson, G., Stone, F. G. A., Abel, E. W., Eds.; Pergamon: New York, 1982; Vols. 3−6.
(5) Wadepohl, H. *Angew. Chem., Int. Ed. Engl.* **1992**, *31*, 247.
(6) Braga, D.; Dyson, P. J.; Grepioni, F.; Johnson, F. G. *Chem. Rev.* **1994**, *94*, 1585.
(7) Salter, A.; Warner, H. *Angew. Chem., Int. Ed. Engl.* **1972**, *11*, 930.
(8) Schildcrout, S. M. *J. Am. Chem. Soc.* **1973**, *95*, 3846.
(9) Kuhlmann, T.; Roth, S.; Roziere, J.; Siebert, W. *Angew. Chem., Int. Ed. Engl.* **1986**, *25*, 105.
(10) Lavrentiev, M. Y.; Köppel, H.; Böhm, M. C. *Chem. Phys.* **1993**, *169*, 85.
(11) Meyer, F. M.; Khan, F. A.; Armentrout, P. B. *J. Am. Chem. Soc.* **1995**, *117*, 9740.
(12) Duncan, M. A. *Int. J. Mass Spectrom.* **2000**, *200*, 545.
(13) Nakajima, A.; Kaya, K. *J. Phys. Chem. A* **2000**, *104*, 176 and references therein.
(14) Weisshaar, J. C. *Acc. Chem. Res.* **1993**, *26*, 213.
(15) Mitchell, S. A.; Hackett, P. A. *J. Chem. Phys.* **1990**, *93*, 7813.
(16) Kurikawa, T.; Takeda, H.; Hirano, M.; Judai, K.; Arita, T.; Nagao, S.; Nakajima, A.; Kaya, K. *Organometallics* **1999**, *18*, 1430.
(17) Hoshino, K.; Kurikawa, T.; Takeda, H.; Nakajima, A.; Kaya, K. *J. Phys. Chem.* **1995**, *99*, 3053.
(18) Weis, P.; Kemper, P. R.; Bowers, M. T. *J. Phys. Chem. A* **1997**, *101*, 8207.
(19) Yasuike, T.; Nakajima, A.; Yabushita, S.; Kaya, K. *J. Phys. Chem. A* **1997**, *101*, 5360.
(20) Yasuike, T.; Yabushita, S. *J. Phys. Chem. A* **1999**, *103*, 4533.
(21) de Heer, W. A. *Rev. Mod. Phys.* **1993**, *65*, 611.
(22) Knickelbein, M. B.; Yang, S.; Riley, S. J. *J. Chem. Phys.* **1990**, *93*, 94.
(23) Lievens, P.; Thoen, P.; Bouvkaert, S.; Bouwen, W.; Vanhoutte, F.; Weidele, H.; Silverans, R. E.; Navarro-Vazquez, A.; von Ragues Schleyer, P. *J. Chem. Phys.* **1999**, *110*, 10316.
(24) Daly, N. R. *Rev. Sci. Instrum.* **1960**, *31*, 264.
(25) Haberland, H. *Clusters of Atoms and Molecules*; Springer-Verlag: Berlin, 1994; p 230.
(26) Nagao, S.; Kurikawa, T.; Miyajima, K.; Nakajima, A.; Kaya, K. *J. Phys. Chem. A* **1998**, *102*, 4495.
(27) Homer, M. L.; Persson, J. L.; Honea, E. C., and Whetten, R. L. *Z. Phys. D* **1991**, *22*, 441.
(28) Loock, H.-P.; Simard B.; Wallin, S.; Linton, C. *J. Chem. Phys.* **1998**, *109*, 8980.